Journal of Fluorescence (2019) 29:587–597
https://doi.org/10.1007/s10895-019-02370-8

ORIGINAL ARTICLE

Rotational Diffusion of Medium Sized 7-[Diethylamino] -2H-1-Benzopyran-2-One Molecule in Alcohols: Study of Temperature and Solvent Viscosity Effect

Anil Kumar[1] · Y. F. Nadaf[2] · C. G. Renuka[3]

Received: 1 February 2019 / Accepted: 19 March 2019 / Published online: 4 April 2019

Abstract
The rotational re-orientations times of the 7-[diethylamino]-2H-1-benzopyran-2-one (7-DHB) dye molecule have been examined in ethanol and octanol solvents when macroscopic solvent viscosity parameter is varied by varying the temperature, by employing the steady-state fluorescence depolarisation and Time-Correlated Single Photon Counting (TCSPC) techniques. Experimental observation shows that 7-DHB probe is experiencing higher friction in octanol compared to ethanol and rotates slower by a factor of 7.3. The hydrodynamic Stokes Einstein's Debye theory (SED) with a stick, slip boundary conditions parameters, quasi-hydrodynamic models (Dote-Kivelson-Schwartz and Geirer-Wirtz) were used to determine mechanical friction and found an interesting towards super slip trend. Dielectric frictional theories of point dipole, Nee-Zwanzig and van der Zwan-Hynes both models fail to describe experimentally observe dielectric friction trends. Evidently, both hydrodynamic and dielectric models failed to explain the examined behavior, even in the qualitative way in alcohols.

Keywords Laser dye · Hydrodynamic theories · Reorientation times · Super slip · Point dipole dielectric theories

Introduction

A good understanding of the molecular correlation functions and correlation times tell us about what's occurring in the immediate neighborhood of the rotating probe molecules. So probe molecular rotations will function as a sensitive probe of molecular structure and molecular dynamics, far more results than translation motion. Thus molecular correlation times provide information on the results of chemical interest like aggregations, solvation, a photochemical process, isomerization and hydrogen bonding [1]. Different types of molecular motion lead to biomolecule collisions of solvent-solute and solute-solute which are a fundamental need for chemical reactions. Understanding the dynamics of molecules solubilized in solvents is vital to get a better appreciation of many chemical reactions that occur in organized media, and inevitably, considerable effort has gone in that direction. The dynamics of solubilized molecules in different polarity of solvents are usually monitored using absorption or fluorescence techniques, and information pertinent to the microenvironment of the probe molecule in the solvent medium is obtained besides the dynamical properties of the probe [2–15]. Study of the rotational and translational diffusion of molecules having potential importance because it leads to understand the dynamic interaction with surrounding molecules, such as solvent-solute interactions. The molecular motions explain restricted or free motions depending on their physical and chemical properties of the surrounding medium. The diffusion motion of large solute molecules is generally described by Brownian motion theories [16]. The hydrodynamic basis for determining the rotational friction encountered by a sphere rotating in a liquid is given by Einstein [17]. This has been subsequently found to be applicable by Einstein in characterizing the Brownian motion of micrometer-sized particles and by Debye describing the dielectric relaxation at the molecular level [18, 19]. The theoretical description of the molecular rotational motion of any probe in the liquid is described by Stokes, Einstein's, Debye and Perrin equation [20], the rotational reorientation

✉ C. G. Renuka
renubub@gmail.com

[1] P.G. Department of Physics, Sri Siddeshwara Govt., First Grade College, Naragund 582207, India

[2] Department of Physics and Research Center, Maharani Science College for Women, Bengaluru 560001, India

[3] Department of Physics, Jnanabharathi campus, Bangalore University, Bengaluru 560056, India

time (τ_r) of the solute is related to the solvent viscosity parameter (η).

A number of investigations have dealt with the study of the dependence of the rotational reorientation times [21–25] on the nature of the solvent, solute size, shape, charges on it, solvent temperature, pressure and solvent composition in binary mixtures to obtain a much better insight into the molecular rotation dynamics. The studies of rotational reorientation dynamics are broadly classified into two categories [26] Firstly, polar probes embedded in charged polar solvents to know how the electrostatic long-range interactions, influence the rotational dynamics of the solute molecules. Secondly, non-polar probes embedded in non-polar or polar solvents to understand the influence solute to solvent size ratio and solute shape. Several important assumptions of the SED's theory [27] explained in the case of the solute-solvent interactions on a microscopic scale molecule, stick and slip boundary conditions parameters on the molecular scale and rotational relaxation times in the solvent on the molecular scales. These assumptions strongly affect the solute-solvent interactions. Information about such interactions is important for various reactions and industrial applications [28, 29].

A molecule rotating in solution experience frictions because of its continuous interactions with its surrounding media and this has been the motivating factor to carry out the experimental rotational reorientation times measurements in solutions. How is this friction modeled? The general approach has been to treat the solute molecule as an ellipsoid moving in a continuous, homogeneous medium characterized by its macroscopic properties such as dielectric constant and viscosity. The friction has both mechanical and dielectric origins. Mechanical friction is modeled by hydrodynamics and the dielectric friction by different continuum theories [30, 31]. The mechanical and dielectric friction contributions to the friction are non-separable because of the electrohydrodynamic coupling [32]. According to experimentalists, the non-separability of the total friction (ζ_{total}) can be written as a contribution of mechanical (ζ_{MeF}) and dielectric (ζ_{DiF}) components.

$$\zeta_{total} = \zeta_{MeF} + \zeta_{DiF} \quad (1)$$

However, elaborate examinations of rotational diffusion have shown the existence of origin of drag about a rotating probe molecule because of specific solvent interactions like hydrogen (H) bonding among the solute-solvent molecules. Such hydrogen bonding formation depends on the substituted functional groups of the solute molecules and the hydrogen bonding solvent molecules [33–38]. Under such conditions, the reorientation time is longer here noticed, as a result of an increase in adequate rotating probe size. A number of investigations on dielectric friction have appeared in the literature [39–51] among which three theories are very important. The first one proposed by Nee and Zwanzing [NZ] [37] treats the solute as a point dipole rotating in a spherical cavity and solvent as a continuum dielectric medium. Second is a semi-empirical approach, which is proposed by van der Zwan and Hynes [40] have shown how the dielectric friction is related to fluorescence Stokes shift response of the solute in the solvent media. The third model proposed by Alavi and Waldeck [43] is analogous to the NZ model wherein the dielectric friction is determined by treating solute as the arbitrary distribution of point charges. Each of these approaches has its own merits and demerits. In this study, we wish to examine issue related to the specific solvent-solute interactions (H-bonding) role on rotation of probes with the aid of acceptable queries. To understand the variation in friction experienced by 7-DHB laser dye in alcohols, when macroscopic solvent viscosity parameter is varied by varying the temperature, we have chosen two alcohols ethanol and octanol whose viscosity are different.

Materials and Experimental Methods

Materials

The laser dye 7-[diethylamino]-2H-1-benzopyran-2-one: (7-DHB) was purchased from Exciton company USA (with 98% purity) and used without further purification. Optimized structure of the studied molecule is shown in Fig. 1. The alcohol solvents such as ethanol and octanol are procured from commercially available local seller (S-D Fine Chemicals Ltd., India) these solvents are of spectroscopic grades and used without further dilution. All the measurements were carried out at 298–343 ± 1 K and the concentration of the solution was maintained in the range of 10^{-6}–10^{-7} M.

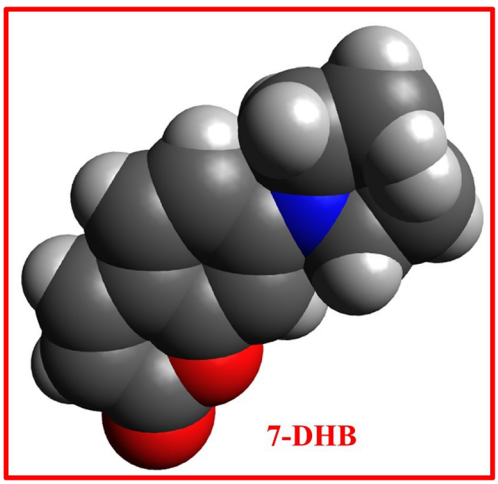

Fig. 1 Optimized geometry structure of 7-DHB laser dye

Experimental Methods

Steady-State Absorption and Fluorescence Measurements

The steady-state absorption spectra of the probe was recorded using Shimadzu UV-1800 spectrophotometer with 1.0-nm resolution. Suitable safety precautions was taken while transferring the solution into the cuvette to prevent moisture absorption of surroundings. The steady-state fluorescence spectra of the probe was recorded using spectrofluorophotometer (Hitachi, model F-2700). While recording the steady-state fluorescence spectra the Xe -lamp was used. While recording the excitation and emission band passes is kept in the range from 0 to 10 nm and to achieve the high fluorescence yield of the probe, the photomultiplier voltage (PM) was set to 400 V.

Steady-State Fluorescence Anisotropy Measurements

Fluorescence anisotropy occurs as a result of the photo selection of fluorophore in the direction of the polarization of the excitation source. The fluorescence anisotropy of solute molecules depends on its own intrinsic property as well as on its environment. In our experiments, fluorescence anisotropies were measured with exciting light polarizer along the Z-direction (laboratory frame) and detecting the components of fluorescence intensity polarized along the Z and Y directions employing a Hitachi F-2700 spectrofluorophotometer, with polarizer accessories (Hitachi Model 650–0155 and 650–0156). The fluorescence intensity component polarized along the Z-direction is referred to as parallel ($I_{\parallel}$), and that polarized along the Y direction is called the perpendicular component ($I_{\perp}$). The steady-state fluorescence anisotropy <r> is characterised by [52].

$$< r >= \left[\frac{I_{\parallel} - G_0 I_{\perp}}{I_{\parallel} + 2G_0 I_{\perp}} \right] \quad (2)$$

where 'G_0' is a correction factor term. It is measured by using horizontally excitation polarized light intensity, and horizontal and vertical polarization intensity of the emitted light. The G_0 correction factor term is given by $G_0 = \left[\frac{I_{HV}}{I_{HH.}}\right]$

Time-Resolved Fluorescence Decay Measurements

Fluorescence decay of 7-DHB dye molecule in alcohol solvents (Fig. 2) was recorded using picosecond laser as an excitation source and a Time-Correlated Single Photon Counting (TCSPC) technique (Edinburgh Instruments, Model: FSP920) along with Hamamatsu PMT is used for fluorescence detector. The excitation source of 408 nm wavelength diode laser (<100 ps, 1MHZ) was used. The device response function was ~260 ps at FWHM. Fluorescence decays measured with an excitation beam of vertically polarized and fluorescence was collected at the magic angle (54.7^0). For all fluorescence detection, the spectral bandwidth is kept at ~7.0 nm. Fluorescence decay data analysis in the present work was done by iterative reconvolution and nonlinear least square method. The fluorescence decay curve analysis was carried out by using the software IBH (DAS-6) based on reconvolution technique.

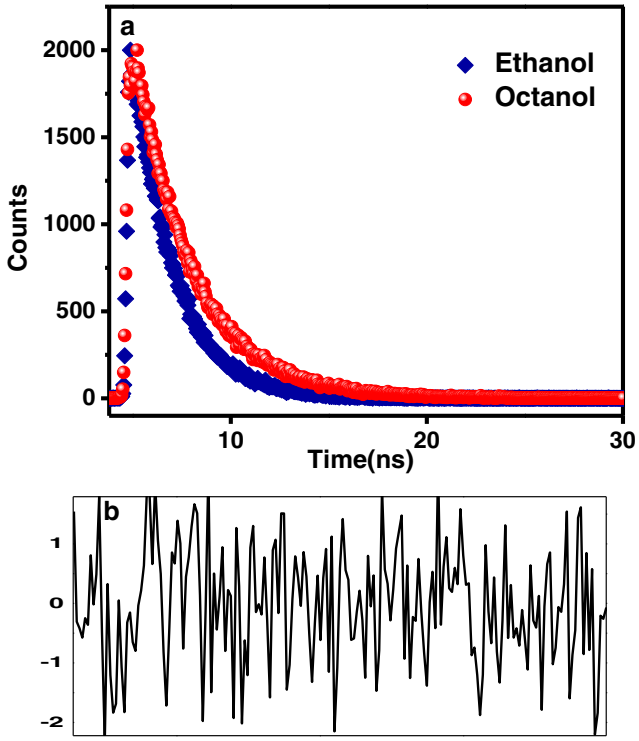

Fig. 2 **a** Fluorescence decay curve of 7-DHB in Ethanol and Octanol solvents at 298 K **b** Residual graph of 7-DHB in one of the studied ethanol solvent

Experimental Rotational Reorientation (τ_r) Measurements

The rotational reorientation times (τ_r) is found from experimentally measured using the relation [52] by

$$\tau_r = \tau_f / \left[\left(\frac{r_o}{\langle r \rangle} \right) - 1 \right] \quad (3)$$

where τ_f – is fluorescence lifetime and r_o – is the limiting anisotropy found in the frozen state of the molecules. r_o - measured by dissolving the probe molecule in glycerol and cooling the solution to a temperature below −18 °C.

Computational Techniques

For the probe, the Time-Dependent Density Functional Theory [TD-DFT] calculations were carried out by using the GAMESS software package [53–55]. Ground state optimized geometry were computed using TD B3LYP/6-31G basis set.

To incorporate both dynamical and non-dynamical correlations affects the most familiar ab-initio methods were used. Vertically excited zero-zero singlet states were computed using the same basis set.

Results and Discussion

Computational Results

Initially, the geometrical optimized structure of the probe is computed using QM-AMI method. In 7-DHB molecule, diethylamine (-N-CH_3) functional group, the bond length of for atom N-12 and C-13 is 1.4866 Å and for atom N-12 and C-15 is 1.4956 Å. For 7-DHB dye, HOMO-LUMO is completely localized over the entire molecule expect on diethyl amine group.

Hydrodynamic Theory

The τ_r–rotational reorientation time relates to η-viscosity of the solvent, according to the Stokes-Einstein's Debye (SED) hydrodynamic theory is given by

$$\tau_r = \left[\frac{\eta V}{KT} \, fC \right] \tag{4}$$

Where K – Boltzmann constant, V- is the van der Waals volume of the probe, T – absolute temperature, f – Shape factor. For non-spherical probes, f is less than one. The amount of variation of 'f' from unity defines the non-spherical natures of the probe, C – boundary conditions that indicate the degree of coupling amid the solvent and solute [56]. The probe molecules shapes are normally included in the model by considering them as either asymmetric or symmetric ellipsoidal. In both constraining cases of hydrodynamic slip and stick conditions for a non-spherical probe, the value of C follow inequalities $0 \leq C \leq 1$ and therefore precise values of 'C' is calculated through the axial ratio of the probe molecules.

To calculate the rotational reorientation times of probe molecule by applying SED theory, the shape factor, stick and slip boundary conditions parameters are determined as follows: In accordance with van der Waals increment method [39], the probe molecular volume of 7-DHB was found to be 203.5$Å^3$. The longest axis (2a) of the probe molecules was taken as the end to end distance. The thickness of the probes C = 1.9 Å for aromatic molecules was taken as half-axis proposed by Fleming et al. [57]. The short in-plane axes (2b) have been found by employing the relation

$$V = \left[\frac{4\pi}{3} \, abc \right] \tag{5}$$

Where V- is the probe volume, the half-axis being a, b and c. The determined van der Waals, axial radii parameters of the probe molecules are 9.33 Å (=a), 2.7 Å (=b) and 1.9 Å (=c). For the estimation of axial, radii 7-DHB probe is modeled as an asymmetric ellipsoid. The coefficients of friction along a, b and c axis with stick boundary condition parameters were found by interpolation of the numerical data of Small and Isenberg [58] whereas slip boundary condition parameters were found by numerical data of Hochstrasser et al. [59]. The diffusion coefficients were determined by the relation of the frictional coefficients ζ_I of the form $D_i = KT/\zeta_i$ by which the rotational reorientation times are determined using the Eq. 1 assuming transition dipole moment is along longest axes

$$\tau_r = \frac{1}{12} \left[\frac{4D_1 + D_2 + D_3}{D_1D_2 + D_2D_3 + D_3D_1} \right] \tag{6}$$

Where D_1, D_2 and D_3 are diffusion coefficients along long, short and out-of-plane axes respectively. The rotational reorientation times of the dye 7-DHB molecule with a stick and slip boundary conditions parameters (using Eq. 6) values are, 176.38 ps and 105.0 ps. Also, f- shape factor (f) and C_{slip} of laser dye 7-DHB are 3.565, 0.595 respectively.

Experimentally obtained steady-state fluorescence anisotropy (<r>), Fluorescence lifetime (τ_f) and Rotational reorientation times (τ_r) of 7-DHB as a function of temperature in ethanol and octanol solvents are tabulated in Tables 1 and 2. The fluorescence lifetimes of the 7-DHB differ in the values, ranges from 3.65 to 3.7 ns in ethanol and 3.71–3.78 ns in octanol. The limiting anisotropy (r_0) values for 7-DHB is found at 0.413. Average values of fluorescence anisotropy's <r> for ethanol and octanol are 0.0066 and 0.04566 respectively. From the values of r_0, <r> and τ_f, the rotation reorientation times were determined (using Eq. 3). The τ_r values decrease with increase in temperature of both the solvents. τ_r values in octanol are larger than ethanol by a factor of 7.3, which implies that 7-DHB laser dye is experiencing higher friction in octanol compared to ethanol. Using Tables 1 and 2 data for 7-DHB laser dye molecule, the plots τ_r v/s η/T least square fitting was performed in both the solvents. A small

Table 1 Steady-State anisotropy <r>, fluorescence life time (τ_f), rotational lifetime (τ_r) of 7-DHB in Ethanol

Temperature/ K	η/mPa s	<r>	τ_f/ ns	τ_r/ ps
298	1.074	0.01	3.70	91.81
303	0.989	0.008	3.69	72.89
313	0.868	0.008	3.68	72.69
323	0.694	0.006	3.68	54.25
333	0.627	0.005	3.66	44.85
343	0.509	0.003	3.65	26.71

Table 2 Steady-State anisotropy <r>, fluorescence life time (τ_f), rotational lifetime (τ_r) of 7-DHB in Octanol

Temperature/ K	η/mPa s	<r>	τ_f /ns	τ_r/ps
298	7.288	0.062	3.78	667.69
303	6.321	0.058	3.76	614.31
313	5.218	0.052	3.76	541.61
323	4.113	0.047	3.75	481.56
333	2.987	0.034	3.73	334.62
343	1.884	0.021	3.71	198.75

negative intercept is noticed in ethanol and a large positive intercept in octanol, representing a non-linear relationship between τ_r v/s η/T in ethanol solvents. So, logarithmic fits were made in both solvents from the τ_r and η/T data relationship obtained results are tabulated in Table 3. From Table 3, it can be found data between τ_r v/s η/T to be nearly linear relation.

Rotational reorientation times (τ_r) calculated with slip (31.27 × η/T) and stick (52.55 × η/T) boundary conditions parameters for the studied probe. A graph of τ_r v/s η/T is plotted for 7-DHB in ethanol and octanol solvents along with slip and stick lines are shown in Fig. 3. The calculated hydrodynamic friction amounts to 61% and 73% of the observed friction for 7-DHB in ethanol and octanol solvents respectively. The difference between experimental and slip rotational times are in the range of 19–47% for ethanol and 17–32% for octanol solvents. The plots of τ_r v/s η/T (Fig. 3) in ethanol and octanol is found to be nearly the same with minor changes is observed. This may be associated with the parent structure of the probe molecule. Note that the experimentally observed reorientation times for 7-DHB laser dye lies between slip and stick lines in an ethanol solvent. The τ_r values for 7-DHB in octanol are observed to be slightly near compared to predicted by the hydrodynamic theory with slip rotational reorientation time. It is interesting to note that experimental and theoretical slip τ_r values initially converges for low temperature and later diverges for higher temperature. Table 3 implies that the probe is experiencing more friction of 37% in octanol than in ethanol solvent.

The SED theories exclusively consider the size of the probe molecules into the study and not considering the size of the solvents. For explaining such observations of size effects, two quasi-hydrodynamic theories by Geirer Wirtz [GW] [60] and Dote-Kivelson Schwartz [DKS] [39] were put forth. GW and DKS take into accounts the sizes of the solute and solvent

Table 3 Relationship between τ_r and η/T obtained from the logarithmic fit of the data in Ethanol, Octanol for the 7-DHB

Solute	Ethanol	Octanol
C-466	$(25.78 \pm 58.30)\left(\frac{\eta}{T}\right)^{0.944}$	$(3.10 \pm 0.27)\left(\frac{\eta}{T}\right)^{0.982}$

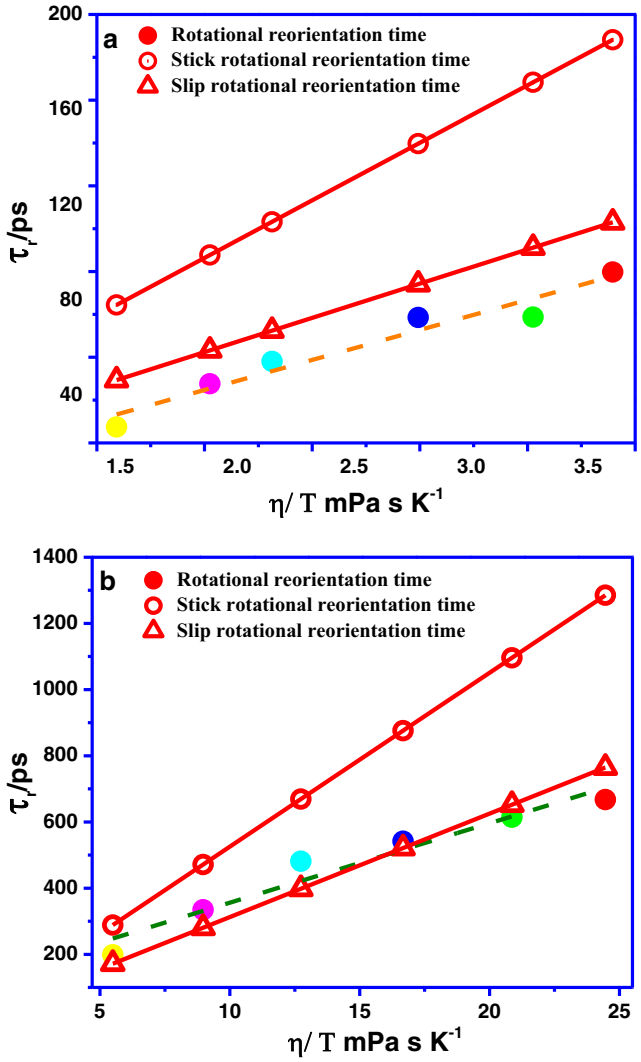

Fig. 3 Plots of rotational time as a function of viscosity/ temperature in **a** Ethanol **b** Octanol of 7-DHB along with theoretical stick and slip rotational reorientation time lines

molecules. GW theory relates to the ratio of solute to solvent size (σ) and is expressed as

$$\sigma = \left[1 + 6\left(\frac{V_s}{V_p}\right)^{1/3} C_0\right]^{-1} \tag{7}$$

where

$$C_0 = \left\{\frac{6\left(\frac{V_s}{V_p}\right)^{1/3}}{\left[1 + 2\left(\frac{V_s}{V_p}\right)^{1/3}\right]^4} + \frac{1}{\left[1 + 4\left(\frac{V_s}{V_p}\right)^{1/3}\right]^3}\right\}^{-1} \tag{8}$$

where V_s – being solvent volume, V_P – probe volume. The equation for the C_{GW} is given by

$$CGW = \sigma\, C_0. \tag{9}$$

The GW theory ignores when relatively weak contact between the solvent and solute, also the cavities of free space formed by the solvent molecules around the probe molecule. The C_{GW} coupling (Using Eqs. 7, 8 and 9) measured value are 0.251 and 0.182 for 7-DHB dye in ethanol and octanol solvents respectively. By comparison of experimental value with reorientation times calculated using GM theory, the model fails to explain the results in a qualitative way. Though GW theory is capable to minimize the non-linear profiles of τ_r v/s η/T plots, it shows underestimated average frictions experienced by probe molecules by factors in the range of 1.37–2.1 for ethanol and 2.9–3.84 for octanol solvents. It is noticed that the larger deviation between experimentally and theoretically calculated reorientation times of the probe. By comparison of reorientation times, the experimental values to calculated using GM theory, the model fails to explain the results in a qualitative way. For understanding this behavior of the probe we use DKS theory.

The solute-solvent coupling parameters, C_{DKS}, and γ, according to DKS model were calculated using the given equations

$$C_{DKS} = \left[1 + \frac{\gamma}{\phi}\right]^{-1} \tag{10}$$

$$\gamma = \frac{\Delta V}{V_p}\left[4\left(\frac{V_s}{V_p}\right)^{2/3} + 1\right] \tag{11}$$

where γ/ϕ – is the ratio of the solvent volume available free to the effective solute size, ϕ – is the ratio of reorientation time obtained using slip hydrodynamic to reorientation time predicted by stick hydrodynamic theory. ΔV – smallest free space volume available per solvent molecule and is given by

$$\Delta V = V_{sm} - V_s \tag{12}$$

where V_{sm} – solvent molar volume /Avogadro number.

The friction calculated from DKS (Using Eqs. 10, 11 and 12) theory to the total friction experienced by the probe was found to be about 40% in ethanol and 75% in octanol solvents. Since DKS theory takes into account the sizes of the dye as well as solvent-free space created by the solvent to calculate the contribution of the friction. The contribution of friction from DKS theory underestimates the observed experimental results by a factor in the range of 3–4.2 and 6.52–8.64 for 7-DHB in ethanol and octanol respectively. The rotational times τ_r for the probe calculated with C_{GW} and C_{DKS} theory, the values of τ_r v/s η/T in alcohol solvents are shown in Fig. 4. From Fig. 4, it is noticed that GW and DKS models fail to explain the results in a qualitative way and underestimate the contribution friction by the probe molecule to a larger extent.

In view of the deviations from experimental results for probe molecule from SED theory and the observed behavior, it becomes imperative to verify for dielectric friction effects.

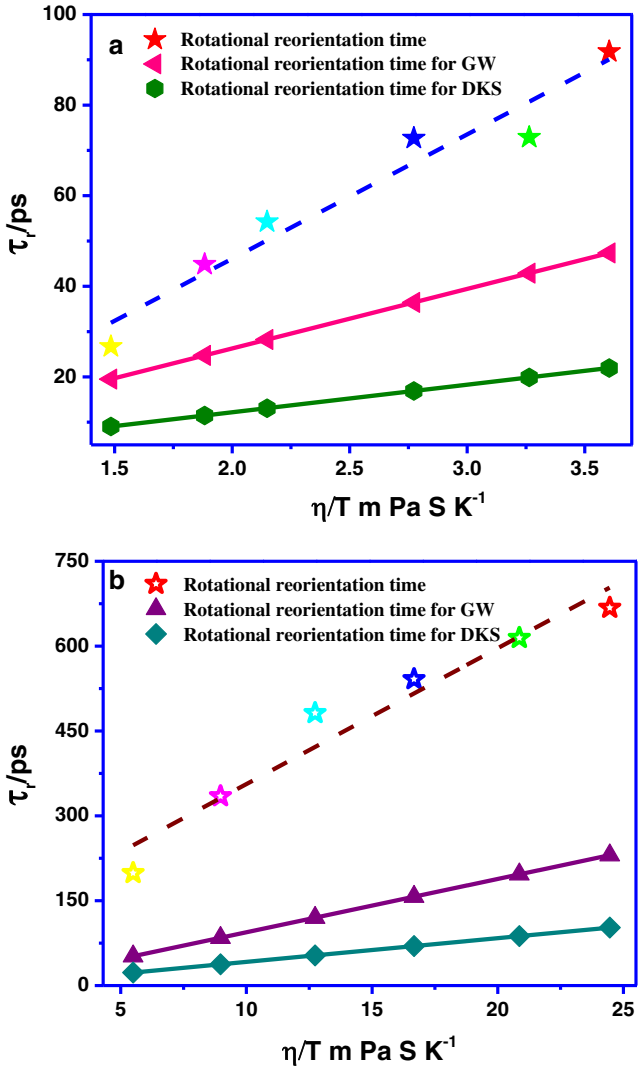

Fig. 4 Plots of rotational time as a function of viscosity/temperature in **a** Ethanol **b** Octanol for 7-DHB with theoretical models of GW and DKS

The observed deviations from the experimental results with those of predicted SED theory have been qualitatively explained using different dielectric friction theories. Among those, some are categorized as continuum models therein the solvents depend strongly on frequency dependent dielectric constant.

Dielectric Friction

When the molecule starts rotating, surrounding media cannot polarise instantaneously and keep in phase with the new orientation of the probe molecule, this lag exerts a retarding force giving rise to rotational dielectric friction on the probe. Two semi-empirical methods have been employed to calculate the contribution of dielectric frictions proposed by NZ and ZH models.

Nee-Zwanzig (NZ) Model

NZ model considers that probe to be a point dipole embedded in a cavity of the radius 'a', solvent as an extended dielectric media described by a frequency dependants of dielectric constants. If μ_e - is the excited state dipole moment, ε_0 – zero frequency dielectric constants and ε_∞ - dielectric constants at high-frequency of the solvent medium and τ_D – Debye relaxations time of the medium. At the limit of zero frequency the dielectric friction (τ_{DF}) of the probe is followed by an equation as

$$\tau_{DF} = \left[\frac{\mu_e^2}{9a^3KT} \frac{(\varepsilon_\infty + 2)^2(\varepsilon_0 - \varepsilon_\infty)}{(2\varepsilon_0 + \varepsilon_\infty)^2} \tau_D \right] \quad (13)$$

The static dielectric properties and τ_D values of studied solvents are tabulated in Table 4. obtained from the literature [61–68]. The dipole moments in an excited state of the probe in alcohols were determined by using Lippert-Mataga equation [24] and shown in Table 5.

Two sets of 'a_0' values have been utilized in the NZ theory (Using Eq. 13) to determine the dielectric frictions contribution. The first set of values of $a_0 = 3.65$ Å found from the van - der-Waals volumes, considering the probe as a spherical molecule and the second set of value are obtained from the half-length of the longest-axes of which values are $a_0 = 9.33$ Å for 7-DHB in both the solvents. Those two sets of a_0 values for a given solute serves as two maximum limits that are employed to determine the contributions of dielectric friction. The contribution of τ_{DF} was calculated with the experimental rotational reorientation time using the relation: $\tau_{DF} = \tau_r^{Expt} - \tau_r^{stick}$ and

Table 4 Dielectric properties of ethanol and octanol solvents used in this study as a function of Temperature

Solvent	Temperature/ K	ε_0 [a]	ε_∞ [b]	τ_D/ps	A X 10^3 /ps K^{-1}
Ethanol	298	7.54	1.848	131.1[c]	129.37
	303	8.05	1.841	133.8	125.66
	313	8.95	1.832	104.0	89.19
	323	10.11	1.822	78.40	60.48
	333	11.15	1.812	55.20	38.69
	343	11.71	1.804	48.80	32.05
Octanol	298	8.48	2.037	1502[d]	1466.76
	303	8.43	2.032	1224	1177.35
	313	8.33	2.025	668.0	624.47
	323	7.71	2.013	481.0	449.91
	333	7.09	2.002	298.0	278.46
	343	4.60	1.989	169.0	163.55

[a, b] Dielectric parameters obtained from interpolation/extrapolation data of Ref. [45, 46]

[c, d] Obtained from the interpolation/ extrapolation data of Ref. [47–52]

Table 5 Excited state dipole moments obtained from the slope of the τ_{DF} v/s A using NZ theory

Solvent	Slope	Intercept	Dipole Moment	
			a = 3.65 Å	a = 9.33 Å
Ethanol	4.9866	32.69218	54.89	24.04
Octanol	39.8451	31.70013	155.16	67.96

$\tau_{DF} = \tau_r^{Expt} - \tau_r^{DKS}$ for the probe, where τ_r^{Expt} – is the experimentally determined rotational reorientation time and τ_r^{stick} – is the theoretical determined rotational reorientation time as per SED theory. To examine the experimentally obtained dielectric friction with that of theoretically calculated dielectric friction, the plot of τ_{DF} v/s A was plotted for the probe, are shown in Fig. 5, where

$$A = \frac{(\varepsilon_\infty + 2)^2(\varepsilon_0 - \varepsilon_\infty)}{(2\varepsilon_0 + \varepsilon_\infty)^2} \tau_D \quad (14)$$

The plots of τ_{DF} v/s A as shown in Fig. 5, it can be inferred that NZ theory underestimates both in ethanol and octanol. From the plots of τ_{DF} v/s A, the obtained slopes are used to determine the excited state dipole moments of 7-DHB and are tabulated in Table 5. From Table 5, it can be noted large dipole moments values are obtained when we use the slopes of τ_{DF} v/s A plots. From Table 4, the 'A' values are 5–11.34 times greater in octanol than ethanol, as per NZ model the τ_{DF} contribution be higher magnitude in octanol. This may be probably the reason for higher dielectric friction experienced by 7-DHB in octanol than ethanol, consequently slower rotation and higher rotational reorientation time.

Van der Zwan Hynes (ZH) Model

The semi-empirical theory as suggested by ZH [40], describes the dielectric friction experienced by the probe in a solvent is related to the solvatochromic Stoke's shift and solvation times (τ_s) and is given by

$$\tau_{DF} = \left[\left(\frac{\mu^2}{\Delta\mu^2} \right) \frac{hc\Delta\nu}{6KT} \tau_s \right] \quad (15)$$

where c - velocity of light in vacuum, τ_s–solvation time, h-Planck's constant and $\Delta\nu$- Stoke's shift (energy difference between 0 and 0 transition for excitation and 0–0 emissions in a given solvent), $\Delta\mu$ – the difference between excited and ground state dipole moment. Solvation dynamics studies [36, 69–74] suggests that the solvent longitudinal relaxation time $\tau_L = \tau_D (\varepsilon_\infty/\varepsilon_0)$ is closely related to solvation time and is nearly independent properties of the probes. So $'\tau_L'$ may be replaced by solvation time.

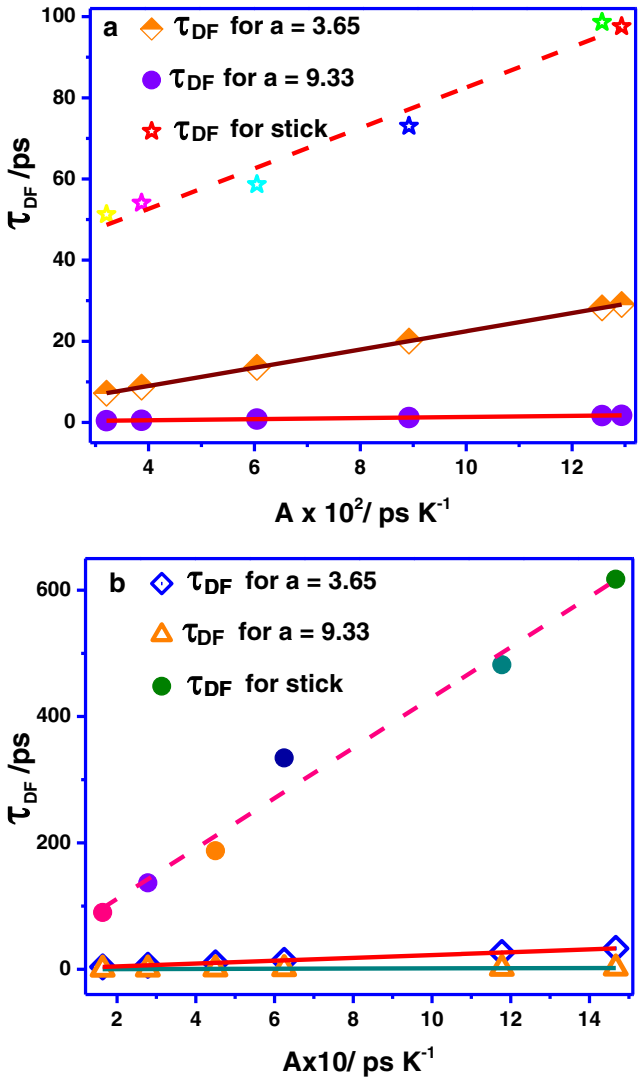

Fig. 5 Rotational time due to dielectric friction τ_{DF} of 7-DHB ($\tau_{DF}= \tau_r^{Obs} - \tau_r^{Stick}$ and $\tau_{DF}= \tau_r^{Obs} - \tau_r^{DKS}$) as a function of A in **a** Ethanol **b** Octanol

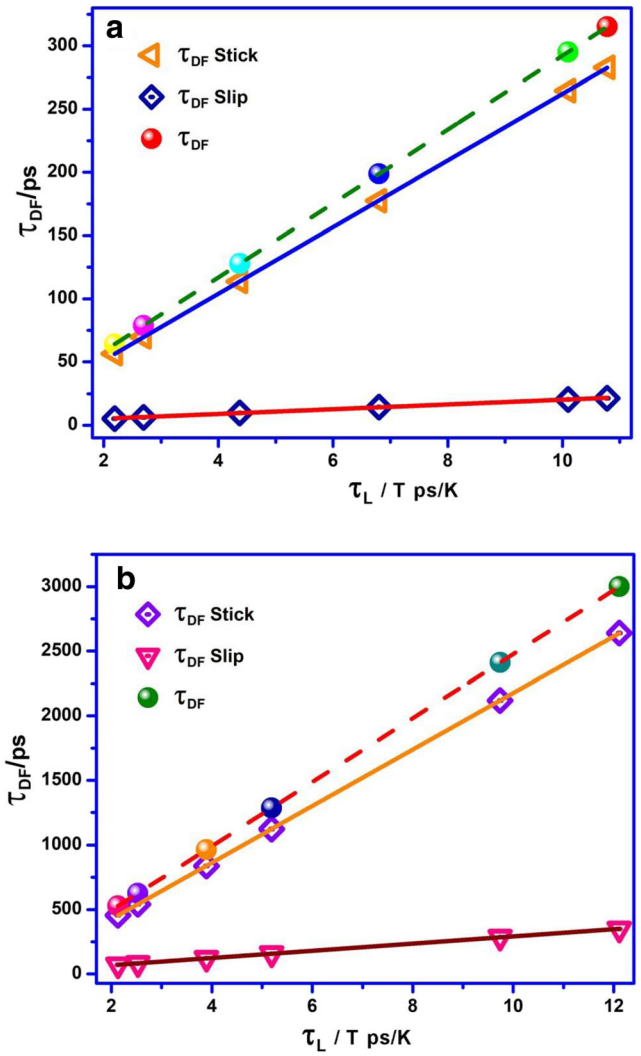

Fig. 6 Rotational time due to dielectric friction τ_{DF} of 7-DHB ($\tau_{DF}= \tau_r^{Obs} - \tau_r^{Stick}$ and $\tau_{DF}= \tau_r^{Obs} - \tau_r^{slip}$) as a function of $\Delta\nu\tau_L$ in **a** Ethanol and **b** Octanol

The dielectric friction (τ_{DF}) contributions were calculated by using the Eq. 15 (ZH model), Stokes shift values used are 4477 cm^{-1} and 3795 cm^{-1}. The τ_{DF} values found from ZH model and experimental results are plotted as a function of τ_L/T as shown in Fig. 6. It can be inferred from plots that the dielectric friction calculated theoretically by ZH model underestimates the observed experimental dielectric friction for $\tau_{DF} = \tau_r^{Expt} - \tau_r^{DKS}$ and is nearly equal $\tau_{DF} = \tau_r^{Expt} - \tau_r^{stick}$, it is exciting to note that $\tau_{DF} = \tau_r^{Expt} - \tau_r^{stick}$ are nearly equal for rotational reorientation at lower temperatures, but it deviates at a higher temperature. The values of $\frac{\mu^2}{\Delta\mu^2}$ are determined by the slopes of τ_{DF} v/s τ_L/T and results are tabulated in Table 6 along with experimentally determined values. The determined $\frac{\mu^2}{\Delta\mu^2}$ values are small the factor of 2.17 for ethanol and higher by a factor of 3.91 for octanol. Similar results found from Dutt et al. [75], in this paper probes size effect is not found in this current work as solute-solvent complexes considerably increases than to the solvent molecules size and hence rotational reorientation times for DPP were found close to the stick boundary conditions in ethylene glycol and decanol solvents because of –NH and –OH of solute and solvents interactions. This work confirms that the increase in the size of solute-solvent complexes, the solute experiences more friction. Also from literature, the rotation dynamics studies of DPP and DMDPP [76, 77] similarly, structured non-polar probes in H-bonding solvents supports strongly our experimental results. Kauffman et al. [78] studies of DPB, and HMS in alcohols series suggests that specific H-bonding interactions in HMS probe and alcohols solvents are important for notable friction. Evidently, both NZ and ZH models also failed to explain the examined behavior, even in the qualitative way [74].

Table 6 Slopes, intercepts and $\mu^2/\Delta\mu^2$ values obtained from the plot of τ_{DF} v/s τ_L/T using the ZH theory in the solvents

Solvent	Slope	Intercept	$\frac{\mu^2}{\Delta\mu^2}$
Ethanol	29.22	−1.705	5.37
Octanol	247.74	−3.183	45.53

To describe dielectric frictions experienced by polar probe molecules embedded in polar solvents, Alavi-Waldeck et al. (AW model) [45] applied point charge distributions (NZ) to the extended charge distributions. AW model is meant to enhance the microscopic effect on dielectric frictions for large solutes and to adequately emphasize the fact that solute with permanent dipole should experience less dielectric friction compared with no permanent dipole. However, in associative solvents like alcohols, it had been futile in modeling the dielectric friction.

Conclusions

The rotational reorientation times of 7-DHB are studied in ethanol and octanol solvents when macroscopic solvent viscosity parameter is varied by varying the temperature. In the SED model the difference between experimental and slip rotational times are in the range of 19–47% for ethanol and 17–32% for octanol solvents. The experimentally observed reorientation times for 7-DHB laser dye lies between slip and stick lines in an ethanol solvent. The τ_r values for 7-DHB in octanol are observed to be slightly near compared to predicted by the hydrodynamic theory with slip rotational reorientation time. The 7-DHB probe is experiencing more friction of 37% in octanol than in ethanol solvent. In view of the deviations from experimental results and the observed behavior of 7-DHB probe molecule from SED, GW and DKS theories, it becomes imperative to verify for dielectric friction effects. The friction contribution of dielectric estimated using NZ theory underestimates the both in ethanol and octanol which is reflected in large dipole moments values than theoretically obtained dipole moments. 'A' values being 5–11.34 times greater in octanol than ethanol results in higher dielectric friction, consequently slower rotation in octanol compared to ethanol. The dielectric friction calculated using ZH model underestimates the observed experimental dielectric friction for $\tau_{DF} = \tau_r^{Expt} - \tau_r^{DKS}$ and is nearly equal $\tau_{DF} = \tau_r^{Expt} - \tau_r^{stick}$. Evidently, both Hydrodynamic and Dielectric models failed to explain the examined behavior, even in the qualitative way in alcohols.

References

1. Mali KS, Dutt GB, Mukherjee T (2008) Rotational diffusion of a nonpolar and a dipolar solute in 1-butyl-3-methylimidazolium hexafluorophosphate and glycerol: interplay of size effects and specific interactions. J Chem Phys 128:054504-1–054504-9. https://doi.org/10.1063/1.2827473
2. Chinna a s P, Jeyabalan S et al (2018) Anthracene-based highly selective and sensitive fluorescent "turn on" chemodosimeter for Hg^{2+}. ACS Omega 3:12341–12348
3. Vandarkuzhali SAA, Natarajan S, Jeyabalan S, Sivaraman G, Singaravadivel S, Muthusubramanian S, Viswanathan B (2018) Pineapple Peel-derived carbon dots: applications as sensor, molecular keypad lock, and memory device. ACS Omega 3:12584–12592
4. Perumal S, Karuppannan S et al (2018) Rhodamine-benzothiazole conjugate as an efficient multimodal sensor for Hg^{2+} ions and its applications of imaging in living cells. New J Chem 42:11665–11672
5. Kumara GGV, Kesavana MP et al Reversible NIR Fluorescent probes for Cu^{2+} ions detection and its Living cell imaging. Sensors Actuators B Chem 255:3235–3247
6. Kumara GGV, Kesavana MP et al (2018) Colorimetric and NIR fluorescence receptors for F− ion detection in aqueous condition and its live cell imaging. Sensors Actuators B Chem 255:3194–3206
7. Ranee SJ, Sivaraman G et al (2018) Quinoline based sensors for bivalent copper ions in living cells. Sensors Actuators B Chem 246:630–637
8. Kumar GGV, Kesavan MP et al (2018) A reversible fluorescent chemosensor for the rapid detection of Hg^{2+} in an aqueous solution: its logic gates behaviour. Sensors Actuators B Chem 273:306–315
9. Elumalai Ramachandran, Somasundaram Anbu Anjugam Vandarkuzhali et al (2018) Phenothiazine based donor - acceptor compounds with SolidState emission in the yellow to NIR region and their highly selective and sensitive detection of cyanide ion in ppb level. Chem Eur J 24:11042–11050
10. Sivaraman G, Iniya M, Anand T, Kotla NG, Sunnapu O, Singaravadivel S, Gulyani A, Chellappa D (2018) Chemically diverse small molecule fluorescent chemosensors for copper ion. Coord Chem Rev 357:50–104
11. Maniyazagan M, Mariadasse R, Nachiappan M, Jeyakanthan J, Lokanath NK, Naveen S, Sivaraman G, Muthuraja P, Manisankar P, Stalin T (2018) Synthesis of rhodamine based organic nanorods for efficient chemosensor probe for Al (III) ions and its biological applications. Sensors Actuators B Chem 254:795–804
12. Omprakash Sunnapu, Niranjan G Kotla et al (2017) Rhodamine-based fluorescent turn-on probe for facile sensing and imaging of ATP in mitochondria. Chem Sel 2: 7654–7658
13. Sufi O Raja, Gandhi Sivaraman et al (2017) Facile synthesis of highly sensitive, red-emitting, Fluorogenic dye for microviscosity and mitochondrial imaging in embryonic stem cells. Chem Sel 2: 4609–4616
14. Omprakash Sunnapu, Niranjan G Kotla et al (2017) Rhodamine based effective hemosensor for chromium(III) and their application in live cell imaging. Sensors Actuators B Chem 246:761–768
15. Shree GJ, Sivaraman G, Siva A, Chellappa D (2019) Anthracene- and pyrene-bearing imidazoles as turn-on fluorescent chemosensor for aluminum ion in living cells. Dyes Pigments 163:204–212
16. Sakthivel P, Sekar K, Sivaraman G, Singaravadivel S (2017) Rhodamine Diaminomaleonitrile conjugate as a novel colorimetric fluorescent sensor for recognition of Cd^{2+} ion. J Fluoresc 27:1109–1115

17. Tao T (1969) Time-dependent fluorescence depolarization and Brownian rotational diffusion coefficients of macromolecules. Biopolymers 8:609–632
18. Einstein A (1956) Investigations in theory of Brownian motion. Dover, New York
19. Kubinyi M, Grofcsik A, Pápai I, Jones WJ (2003) Rotational reorientation dynamics of nile blue a and oxazine 720 in protic solvents. Chem Phys 286:81–96. https://doi.org/10.1016/S0301-0104(02)00908-4
20. Zhou P, Song P, Liu J, Shi Y, Han K, He G (2008) Rotational reorientation dynamics of oxazine 750 in polar solvents. J Phys Chem A 112:3646–3655. https://doi.org/10.1021/jp7120998
21. Raikar US, Renuka CG, Nadaf YF, Mulimani BG, Karguppikar AM (2006) Rotational diffusion and solvatochromic correlation of coumarin 6 laser dye. J Fluoresc 16:847–854. https://doi.org/10.1007/s10895-006-0126-4
22. Gangamallaiah V, Dutt GB (2012) Rotational diffusion of nonpolar and ionic solutes in 1-Alkyl-3- methylimidazolium bis (trifluoromethylsulfonyl) imides: is solute rotation always influenced by the length of the alkyl chain on the imidazolium cation? J Phys Chem B 116:12819–12825. https://doi.org/10.1021/jp307959z
23. Prabhu SR, Dutt GB (2014) Rotational diffusion of nonpolar and charged solutes in propylammonium nitrate-propylene glycol mixtures: does the organized structure of the ionic liquid influence solute rotation? J Phys Chem B 118:2738–2745. https://doi.org/10.1021/jp501343k
24. Prabhu SR, Dutt GB (2014) Rotational diffusion of nondipolar and charged solutes in alkyl-substituted imidazolium triflimides: effect of C2 methylation on solute rotation. J Phys Chem B 118:9420–9426. https://doi.org/10.1021/jp5055155
25. Nadaf YF, Renuka CG, Raikar US (2013) Temperature-dependent reorientation dynamics of laser dyes in alkane and alcohol solvents. Can J Phys 91:677–681
26. Sharma A, Ghorai PK (2018) Effect of alcohols on the structure and dynamics of [BMIM][PF6] ionic liquid: A combined molecular dynamics simulation and Voronoi tessellation investigation. J Chem Phys 148:204514–1–204514-11. https://doi.org/10.1063/1.5008439
27. Nadaf YF, Renuka CG (2015) Analysis of rotational diffusion of coumarin laser dyes. Can J Phys 93:3–6
28. Dutt GB, Ghanty TK (2004) Rotational dynamics of nondipolar probes in butanols: correlation of reorientation times with solute-solvent interaction strengths. J Phys Chem A 108:6090–6095. https://doi.org/10.1021/jp048601q
29. Osman D, Erol A (2009) Apparent molar volumes and isentropic compressibilities of benzyltrialkylammonium chlorides in water at (293.15, 303.15, 313.15,323.15 and 333.15) K. J Chem Thermodyn 41:911–915
30. Erol A, Osman D (2010) Apparent molar volumes and isentropic compressibilities of benzene sulfonates and naphthalene sulfonates in aqueous solution at (293.15, 303.15, 313.15,323.15 and 333.15) K. J Chem Eng Data 55(2):947–952
31. Hay CE, Marken F, Blanchard GJ (2010) Solvent-dependent changes in molecular reorientation dynamics: the role of solvent-solvent interactions. J Phys Chem A 114:4957–4962. https://doi.org/10.1021/jp912217r
32. Jin H, Baker GA, Arzhantsev S, Dong J, Maroncelli M (2007) Solvation and rotational dynamics of coumarin 153 in ionic liquids: comparisons to conventional solvents. J Phys Chem B 111:7291–7302. https://doi.org/10.1021/jp070923h
33. Kumar PV, Maroncelli M (2000) The non-separability of dielectric and mechanical friction in molecular systems: a simulation study. J Chem Phys 12:5370–5381. https://doi.org/10.1063/1.481107
34. Prabhu SR, Dutt GB (2015) Rotational diffusion of charged and nondipolar solutes in ionic liquid-organic solvent mixtures: evidence for stronger specific solute-solvent interactions in presence of organic solvent. J Phys Chem B 119:10720–10726. https://doi.org/10.1021/acs.jpcb.5b06297
35. Dutt GB (2005) Molecular rotation as a tool for exploring specific solute-solvent interactions. Chem Phys Chem 6:413–418. https://doi.org/10.1002/cphc.200400337
36. Guo J, Han KS, Mahurin SM, Baker GA, Hillesheim PC, Dai S, Hagaman EW, Shaw RW (2012) Rotational and translational dynamics of rhodamine 6G in a pyrrolidinium ionic liquid: a combined time-resolved fluorescence anisotropy decay and NMR study. J Phys Chem B 116:7883–7890
37. Tiwari AK, Sonu SSK (2014) Effect of hydroxyl group substituted spacer group of cationic gemini surfactants on solvation dynamics and rotational relaxation of coumarin-480 in aqueous micelles. J Phys Chem B 118:3582–3592. https://doi.org/10.1021/jp4069703
38. Nee TW, Zwanzig R (1970) Theory of dielectric relaxation in polar liquids. J Chem Phys 52:6353–6363. https://doi.org/10.1063/1.1672951
39. Hu C, Zwanzig R (1974) Rotational friction coefficients for spheroids with the slipping boundary condition. J Chem Phys 60:4354–4357
40. Madden P, Kivelson D (1982) Dielectric friction and molecular reorientation. J Phys Chem 86:4244–4256. https://doi.org/10.1021/j100218a031
41. Van Der Zwan G, Hynes JT (1985) Time-dependent fluorescence solvent shifts, dielectric friction, and nonequilibrium solvation in polar solvents. J Phys Chem 89:4181–4188. https://doi.org/10.1021/j100266a008
42. Ben-Amotz D, Drake JM (1988) The solute size effect in rotational diffusion experiments: a test of microscopic friction theories. J Chem Phys 89:1019–1029. https://doi.org/10.1063/1.455253
43. Simon JD, Thompson PA (1990) Spectroscopy and rotational dynamics of oxazine 725 in alcohols: a test of dielectric friction theories. J Chem Phys 92:2891–2896. https://doi.org/10.1063/1.457936
44. Alavi DS, Hartman RS, Waldeck DH (1991) A test of continuum models for dielectric friction. Rotational diffusion of phenoxazine dyes in dimethylsulfoxide. J Chem Phys 94:4509–4520. https://doi.org/10.1063/1.460606
45. Goudar R, Gupta R, Kulkarni GU, Inamdar SR (2015) Rotational diffusion of a new large non polar dye molecule in alkanes. J Fluoresc 25:1671–1679. https://doi.org/10.1007/s10895-015-1654-6
46. Horng ML, Gardecki JA, Maroncelli M (1997) Rotational dynamics of coumarin 153: time-dependent friction, dielectric friction, and other nonhydrodynamic effects. J Phys Chem A 101:1030–1047. https://doi.org/10.1021/jp962921v
47. Maroncelli M (1997) Continuum estimates of rotational dielectric friction and polar solvation. J Chem Phys 106:1545–1555. https://doi.org/10.1063/1.473276
48. Dutt GB, Raman S (2001) Rotational dynamics of coumarins: an experimental test of dielectric friction theories. J Chem Phys 114:6702–6713. https://doi.org/10.1063/1.1357797
49. Mannekutla JR, Inamdar SR, Mulimani BG, Savadatti MI (2010) Rotational diffusion of Coumarins: a dielectric friction study. J Fluoresc 20:797–808. https://doi.org/10.1007/s10895-010-0606-4
50. Inamdar SR, Mannekutla JR, Mulimani BG, Savadatti MI (2006) Rotational dynamics of nonpolar laser dyes. Chem Phys Lett 429:141–146. https://doi.org/10.1016/j.cplett.2006.08.020
51. Hughes RM, Mutzenhardt P, Bartolotti L, Rodriguez AA (2008) Experimental and theoretical analysis of the reorientational dynamics of fullerene C70 in various aromatic solvents. J Phys Chem A 112:4186–4193. https://doi.org/10.1021/jp800027j
52. Gayathri BR, Mannekutla JR, Inamdar SR (2008) Rotational diffusion of coumarins in alcohols: a dielectric friction study. J Fluoresc 18:943–952

53. Lackowicz JR (1983) Principles of fluorescence spectroscopy. Plenum, New York
54. Schmidt MW, Baldridge KK, Boatz JA, Elbert ST, Gordon MS, Jensen JH, Koseki S, Matsunaga N, Nguyen KA, Su S, Windus TL, Dupuis M, Montgomery JA (1993) General atomic and molecular electronic structure system. J Comput Chem 14:1347–1363
55. Renuka CG, Shivashankar K, Boregowda P, Bellad SS, Muregendrappa MV, Nadaf YF (2017) An experimental and computational study of 2-(3-Oxo3H-benzo[f] chromen-1-ylmethoxy)-benzoic acid methyl Ester. J Solut Chem 46:1535–1555. https://doi.org/10.1007/s10953-017-0661-4
56. Renuka CG, Nadaf YF, Sriprakash G, Rajendra Prasad S (2018) Solvent dependence on structure and electronic properties of 7-(Diethylamino) – 2H -1- Benzopyran −2- one (C-466) laser dye. J Fluoresc 28:839–854. https://doi.org/10.1007/s10895-018-2249-9
57. Edward JT (1970) Molecular volumes and the stokes-Einstein equation. J Chem Educ 47:261–270. https://doi.org/10.1021/ed047p2613/1.1680910
58. Fleming GR (1986) Chemical applications of ultrafast spectroscopy. Oxford University Press, London
59. Small EW, Isenberg I (1977) Hydrodynamic properties of a rigid macromolecule: rotational and linear diffusion and fluorescence anisotropy. Biopolymers 16:1907–1928
60. Sension RJ, Hochstrasser RM (1993) Comment on: rotational friction coefficients for ellipsoids and chemical molecules with slip boundary conditions. J Chem Phys 98:2490
61. Gierer VA, Wirtz K (1953) Molecular theory of microreiberation. Z Naturforschg 8A:532–538
62. Dean JA (1999) Lange's handbook of chemistry. Mcgraw-Hill, Inc, New York
63. Bartnikas R (1994) Engineering dielectrics. PA ASTMA, Philadelphia
64. Dannhauser W (1968) Dielectric relaxation in isomeric Octyl alcohols. J Chem Phys 48:1918–1923. https://doi.org/10.1063/1.1668990
65. ShyhGang S, Simon JD (1988) The importance of vibrational motion and solvent diffusional motion in excited state intramolecular electron transfer reactions. J Chem Phys 89:908–919. https://doi.org/10.1063/1.455214
66. Dutt GB, Doraiswamy S, Periasamy N, Venkataraman B (1990) Rotational reorientation dynamics of polar dye molecular probes by picosecond laser spectroscopic technique. J Chem Phys 93:8498–8513. https://doi.org/10.1063/1.459288
67. Dutt GB, Ghanty TK (2003) Rotational dynamics of nondipolar probes in associative solvents: modeling of hydrogen bonding interactions using the extended charge distribution theory of dielectric friction. J Chem Phys 118:4127–4133. https://doi.org/10.1063/1.1540092
68. Garg SK, Smyth CP (1966) Microwave absorption and molecular structure in liquids. The three dielectric dispersion regions of the normal primary alcohols. J Phys Chem 69:1294–1301
69. Philips LA, Webb SP, Clark JH (1985) High pressure studies of rotational reorientation dynamics: the role of dielectric friction. J Chem Phys 83:5810–5821. https://doi.org/10.1063/1.449661
70. Bagchi B, Jana B (2010) Solvation dynamics in dipolar liquids. Chem Soc Rev 39:1936–1954. https://doi.org/10.1039/b902048a
71. Rosenthal SJ, Jimenez et al (1994). Solvation dynamics in methanol: experimental and molecular dynamics simulation studies. J Mol Liq 60:25–56. https://doi.org/10.1016/0167-7322(94)00738-1
72. Simon JD (1988) Time-resolved studies of solvation in polar media. Acc Chem Res 21:128–134. https://doi.org/10.1021/ar00147a006
73. Yevheniia S, François-Alexandre M et al (2017) Solvation dynamics and rotation of coumarin 153 in a new ionic liquid/molecular solvent mixture model: [BMIM][TFSI]/propylenecarbonate. J Mol Liq 226:48–55. https://doi.org/10.1016/j.molliq.2016.10.00
74. Zhang XX, Liang M, Ernsting NP, Maroncelli M (2013) Complete solvation response of coumarin 153 in ionic liquids. J Phys Chem B 117:4291–4304. https://doi.org/10.1021/jp305430a
75. Dutta GB, Rama Krishna G (2001) Rotational dynamics of coumarins in nonassociative solvents: point dipole versus extended charge distribution models of dielectric friction. J Chem Phys 115:4732–4741. https://doi.org/10.1063/1.1395563
76. Dutt GB (2000) Rotational dynamics of non-dipolar probes in alkane–alkanol mixtures: microscopic friction on hydrogen bonding and non-hydrogen bonding solute molecules. J Chem Phys 113:11154–11158
77. Wiemers K, Kauffman JF (2000) Dielectric friction and rotational diffusion of hydrogen bonding solutes. J Phys Chem 104:451–457
78. Dutt GB, Srivastavoy VJP, Sapre AV (1999) Rotational dynamics of pyrrolopyrrole derivatives in glycerol: a comparative study with alcohols. J Chem Phys 111:9705–9710